Measurements of Phase-matching Spectral Phase and Domain Period Distribution by Nonlinear Spectral Interferometry

Chia-Lun Tsai,[1,*] Ming-Chi Chen,[1] Jui-Yu Lai,[1,2] and Shang-Da Yang[1]
[1]Institute of Photonics Technologies, National Tsing Hua University, Hsinchu 30013, Taiwan
[2]HC Photonics Corp., R&D Division, 4F, No.2, Technology Rd. V, Hsinchu Science Park, Hsinchu 30078, Taiwan
Corresponding author: tsaichalun@gmail.com

Abstract: Phase-mating spectral phases of aperiodic quasi-phase matched gratings are experimentally measured by nonlinear spectral interferometry and microscopic images, respectively. The former enables accurate reconstruction of domain length distributions with 810-μm resolution.

I. INTRODUCTION

Aperiodic quasi-phase matching (QPM) gratings have been used in applications such as few-cycle mid infrared pulse generation [1] and multi-channel packet routing in telecommunications. Since the output pulse shape and domain period distribution $\Lambda(x)$ depend on the complex phase-matching (PM) spectrum $H(\Omega)$ of the QPM grating, experimental techniques to measure $H(\Omega)$ are desirable. We had successfully measured the phase of $H(\Omega)$ by nonlinear spectral interferometry (NLSI) for the first time (to the best of our knowledge) [2]. In this work, we analyzed $H(\Omega)$ and $\Lambda(x)$ of aperiodically poled $LiNbO_3$ (A-PPLN) measured by NLSI and microscopic images (of HF-etched surfaces), respectively. It is found that NLSI is fast, nondestructive, free of the errors due to image concatenation (artificial random duty cycle error) and inhomogeneous poling over the cross-section (Fig. 1).

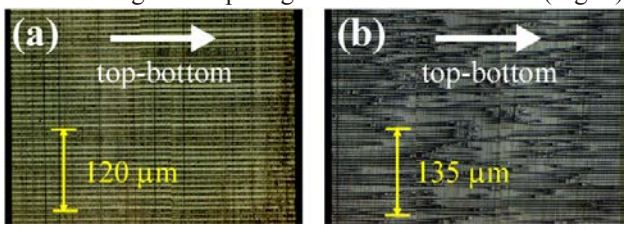

Fig. 1. Microscopic cross-sectional images of PPLN samples with (a) homogeneous, and (b)inhomogeneous poling. Dark regions stand for the inverted domains.

II. THEORY AND EXPERIMENTAL RESULTS

NLSI roots in spectral interferometry (SI) [3], while the signal and reference waves come from second-harmonic generation (SHG) of a common fundamental field of spectral envelope $A(\omega)$ passing through a test QPM grating and a reference thin nonlinear crystal with PM responses $H(\Omega)$ and $H_r(\Omega)$, respectively [2]. The spectral envelopes of signal and reference waves are $A_s(\Omega)=P_{NL}(\Omega)\times H(\Omega)$ and $A_r(\Omega)=P_{NL}(\Omega)\times H_r(\Omega)$, where $P_{NL}(\Omega)=A(\omega)\otimes A(\omega)$ represents the nonlinear polarization spectrum of $A(\omega)$. The fringe density of second-harmonic interferogram $S(\Omega)$ depends on $\Delta\psi(\Omega)=\angle H(\Omega)-\angle H_r(\Omega)=\psi(\Omega)-\psi_r(\Omega)$, independent of the phase of $P_{NL}(\Omega)$. The phase difference function $\Delta\psi(\Omega)$ is equal to the desired $\psi(\Omega)$ if the reference crystal is sufficiently thin such that $\psi_r(\Omega)$ is nearly constant within the frequency range of interest. Since measuring the SHG yield as a function of input wavelength provides $|H(\Omega)|$, the domain reversal pattern $g(x)$ can be obtained by changing the variable from Ω to Δk with known dispersion [4] and Fourier transform (FT) of the complex PM response $H(\Delta k)$. The FT relation implies that a higher spatial resolution of $g(x)$ needs a broader bandwidth of light source.

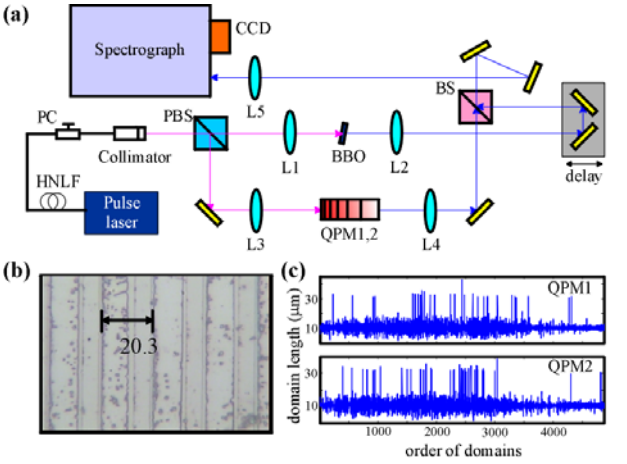

Fig. 2. (a) The NLSI setup. HNLF: Highly nonlinear fiber. PC: Polarization controller. PBS: Polarization beamsplitter. L#: Lens. BS: Beamsplitter. (b) A microscopic image of QPM1 with 10 domains. (c) The global domain length distributions of QPM1 and QPM2 obtained by concatenating 620 and 623 microscopic images, respectively.

Figure 2(a) shows the experimental setup of NLSI. A mode-locked fiber laser produces 50 MHz, 300 fs, 1.4 mW pulses at 1560 nm. The -10 dB bandwidth of the fundamental spectrum is broadened to 79 nm (1527-1606 nm) by 15-m-long highly nonlinear fiber (HNLF). The p-wave and s-wave components are separated by a polarization beam-splitter (PBS), focused into a 1-mm-thick type-1 BBO reference crystal and a 49.5-mm-long A-PPLN crystal with different types of QPM gratings (HC Photonics) to generate the SHG reference and signal pulses, respectively. The domain period distributions $\Lambda(x)$

of 49.5-mm-long QPM1 and QPM2 are linear and quadratic functions monotonically decreasing from 20.4 μm to 19.9 μm, respectively. The two SHG pulses are recombined by a beam-splitter, focused into a spectrograph (iHR550, Jobin Yvon), and recorded by a CCD array to get the interferogram $S(\Omega)$.

Figure 2(b) is a microscopic image of 8+ domains of QPM1, from which we can measure the local domain lengths. The global domain length distributions of QPM1, QPM2 are obtained by combining the results of ~620 images taken from each of the two QPM gratings [Fig. 2(c)]. In addition to the majority lengths around 10 μm, there are 30 and 40 "long domains" (~30 μm) out of the total 4925 and 4948 "mask-defined" domains in QPM1 and QPM2, respectively. This is attributed to the failure of domain inversion during the poling process such that three neighboring mask-defined domains actually merge into a 3-time-longer domain.

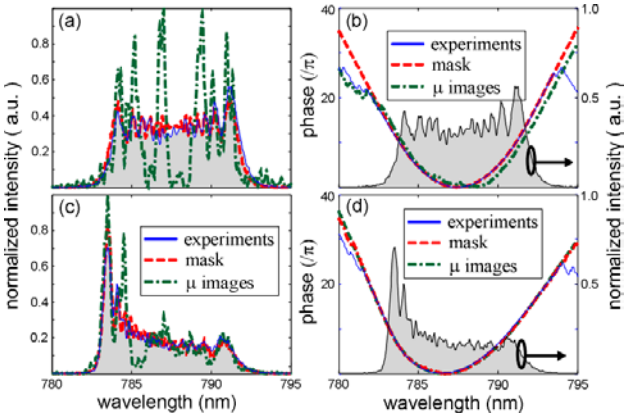

Fig. 3. PM responses obtained by experiments (solid), mask functions (dashed), and microscopic images (dashed-dotted), respectively. (a) Power spectrum of QPM1. (b) Spectral phase of QPM1. (c) Power spectrum of QPM2. (d) Spectral phase of QPM2.

Figures 3(a) and 3(c) show the PM power spectra of QPM1 and QPM2 obtained by three methods: (1) wavelength-scanning SHG experiment (shaded), (2) FT of the mask-defined $g(x)$ (dashed), (3) FT of the microscopically imaged $g(x)$ (dashed dotted), respectively. It is evident that the artificial random duty cycle error due to concatenating a large number of microscopic images may result in a strongly distorted PM power spectrum. The curves in Figs 3(b) and 3(d) represent the PM spectral phases of QPM1 and QPM2 obtained by NLSI experiment ψ_{exp} (solid), mask function ψ_m (dashed), and microscopic images ψ_μ (dashed-dotted), respectively. The root-mean-square (rms) phase error [2] between ψ_{exp} and ψ_m are 0.36π (QPM1) and 0.31π (QPM2), smaller than 1.46π (QPM1) and 0.32π (QPM2) between ψ_μ and ψ_m.

Figure 4 shows the domain period functions $\Lambda_{exp}(x)$ and $\Lambda_\mu(x)$ measured by (NLSI and wavelength-scanning SHG) experiments and microscopic images, respectively. The spatial resolution (810 μm) enabled by the spectral window (783-792 nm) of the NLSI interferograms can tell the slowly-varying (in millimeters) domain periods due to mask design or undesired pattern definition error, but is insufficient to identify sub-resolution structures (e.g. the long domains due to inversion failure and the random duty cycle error). It is found that ultra-broadband fundamental light sources covering 1367-1858 nm (58 THz) and 1105-2742 nm (162 THz) are required to resolve 30-μm long domains and 10-μm typical domains in our sample, respectively. As a result, we reduced the spatial resolution of the raw domain period functions to ~800 μm by piecewise average. As shown in Figs 4(a) and 4(b), $\Lambda_{exp}(x)$ and $\Lambda_\mu(x)$ of QPM1 and QPM2 well resolve the linear and quadratic trends of $\Lambda_m(x)$ defined by the masks. The bumpy $\Lambda_\mu(x)$ primarily arise from the 0.2-μm uncertainty in positioning the domain boundaries in microscopic images. The maximum, mean, and standard deviation of the period difference $\Delta\Lambda(x)=|\Lambda_{exp}(x)-\Lambda_\mu(x)|$ are 305 nm, 41 nm, 58 nm (QPM1) or 238 nm, 31 nm, 39 nm (QPM2), respectively.

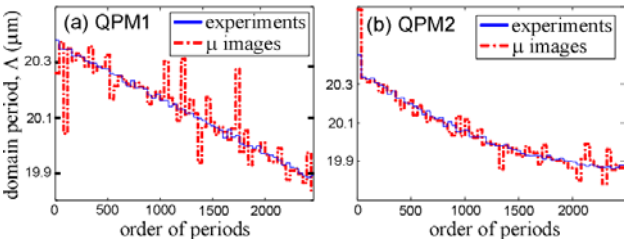

Fig. 4. Domain period distributions measured by experiments (Λ_{exp}, solid) and microscopic images (Λ_μ, dashed-dotted), respectively.

III. CONCLUSIONS

We analyzed the experimentally measured phase-matching spectral phases and domain period distributions of aperiodic QPM gratings by nonlinear spectral interferometry (NLSI) and microscopic images, respectively. It is found that NLSI is fast, nondestructive, free of artificial random duty cycle error due to image concatenation, and can directly measure the region actually accessed by the optical beams (instead of the crystal surface). This material is based on research supported by the National Science Council of Taiwan under grants NSC-99-2120-M-007-010, and NSC-100-2221-E-007-093-MY3.

REFERENCES

[1] C. Heese, C. R. Phillips, L. Gallmann, M. M. Fejer, U. Keller, "Ultrabroadband, highly flexible amplifier for ultrashort midinfrared laser pulses based on aperiodically poled Mg:LiNbO3," *Opt. Lett.*, **35**, pp. 2340-2342, 2010.

[2] Ming-Chi Chen, Shang-Da Yang, "Measurement of phase-matching spectral phase by nonlinear spectral phase interferometry," *IEEE Photonics Conf.,* Arlington, Virginia (USA), October 2011, pp. 383-384.

[3] L. Lepetit, G. Chériaux, M. Joffre, "Linear techniques of phase measurement by femtosecond spectral interferometry for applications in spectroscopy," *J. Opt. Soc. Am. B*, **12**, pp. 2467-2474, 1995.

[4] O. Gayer, Z. Sacks, E. Galun, and A. Arie, "Temperature and wavelength dependent refractive index equations for MgO-doped congruent and stoichiometric $LiNbO_3$," *Applied Physics B*, **91**, pp. 343-348, 2008.